

High-order 3D Voronoi tessellation for identifying isolated galaxies, pairs and triplets

A. Elyiv,^{1*} O. Melnyk^{1,2} and I. Vavilova^{1,3}

¹Main Astronomical Observatory, Academy of Sciences of Ukraine, 27 Akademika Zabolotnoho St., 03680 Kyiv, Ukraine

²Astronomical Observatory, Kyiv National University, 3 Observatorna St., 04053 Kyiv, Ukraine

³Space Research Institute, National Space Agency of Ukraine, National Academy of Sciences of Ukraine, 40 Akademika Glushkova av., 03680 Kyiv, Ukraine

Accepted 2008 October 25. Received 2008 October 5; in original form 2008 April 8

ABSTRACT

A geometric method based on the high-order 3D Voronoi tessellation is proposed for identifying single galaxies, pairs and triplets. This approach allows us to select small galaxy groups and isolated galaxies in different environments and to find the isolated systems. The volume-limited sample of galaxies from the Sloan Digital Sky Survey Data Release 5 spectroscopic survey was used. We conclude that in such small groups as pairs and triplets, segregation by luminosity is clearly observed: galaxies in isolated pairs and triplets are on average two times more luminous than isolated galaxies. We consider the dark matter content in different systems. The median values of mass-to-luminosity ratio are $12 M_{\odot}/L_{\odot}$ for the isolated pairs and $44 M_{\odot}/L_{\odot}$ for the isolated triplets, and 7 (8) M_{\odot}/L_{\odot} for the most compact pairs (triplets). We also found that systems in denser environments have greater rms velocity and mass-to-luminosity ratio.

Key words: galaxies: general – galaxies: kinematics and dynamics – dark matter.

1 INTRODUCTION

The physical properties of galaxies depend on the formation conditions and evolution. In addition to intrinsic evolution, galaxies are exposed to environmental influence (see, among others, Dressler 1980; Lewis et al. 2002; Gomez et al. 2003; Einasto et al. 2003; Blanton et al. 2005; Martinez & Muriel 2006; Weinmann et al. 2006; Park et al. 2007, 2008). The density of galaxies (number of galaxies per volume unit) or luminosity density and the number of galaxies in group/cluster or distance to the nearest galaxy are often assumed to reflect the environment. The influence of an environment can be found up to 1 Mpc and even farther (Kauffmann et al. 2004; Blanton et al. 2005; Park et al. 2007, 2008), where small galaxy groups are observed. The study of ‘environmental effects’ in such poor galaxy groups is helpful for understanding the galaxy evolution on intermediate scales between isolated galaxies and rich groups/clusters.

The isolated galaxies that have not sufficiently undergone the influence of environment allow us to consider them as ‘autonomous laboratories’ for studying the evolutionary processes in the galaxies. Individual properties of isolated galaxies (mass, luminosity, morphology, colour-index, etc.) can be regarded as the standard when studying galaxies in different environments (see e.g. Karachentseva 1973, hereafter KIG; Prada et al. 2003; Reda et al. 2004; Stocke et al. 2004; Verley et al. 2007). To study galaxy properties in different environments, it is also important to define the galaxy’s isolation

degree which can be described by some parameter. For example, Karachentsev & Kasparova (2005) used the tidal index for each galaxy to study global properties of nearest galaxies in different environments. Verley et al. (2007) quantified the isolation degree of KIG galaxies by two parameters: local number density and tidal strength.

It is known that with the increase in galaxy system richness from individual galaxies to clusters, their mass increases more quickly than luminosity (Karachentsev 1966; Girardi et al. 2002). The dark matter in small groups seems to be distributed in the whole volume of the system in the case of compact groups and to be concentrated in the halo of individual galaxies in the case of loose groups (Mulchaey et al. 2003; Melnyk & Vavilova 2006; Da Rocha, Ziegler & Mendes de Oliveira 2008). At the same time, the amount of dark matter in galaxy groups is not enough for the standard cosmological model (Makarov & Karachentsev 2007).

As a rule, for identifying groups by different selection methods, the principle of overdensity in comparison with the background is used. The richer the group population, the stronger the overdensity and therefore the more likely that such a group is physically bound. Identification of poor groups depends strongly on the limiting parameters of the method. These systems can be easily confused with the random physically unbound systems. For this reason, many authors prefer to study rich groups/clusters only. That is why the elaboration of the reliable methods for identifying small groups will allow us to pay more attention to these structures.

Karachentsev (1972, 1987), Karachentseva, Karachentsev & Sherbanobsky (1979) and Karachentseva & Karachentsev (2000)

*E-mail: elyjiw@ukr.net

used a 2D method for pair and triplet selection taking into account the isolation degree in comparison with the foreground and background. The environment of each pair and triplet was inspected using Palomar Observatory Sky Survey (POSSI and POSSII) and European Southern Observatory SERC plates. This method selects effectively the isolated systems, which are compact in projection with characteristic distance between galaxies $R \sim 50$ and 100 kpc. With the appearance of the large data bases and surveys [Lyon–Meudon Extragalactic Database (LEDa), NASA/IPAC Extragalactic Database (NED), Sloan Digital Sky Survey (SDSS), The Center for Astrophysics Redshift Survey 2 (CfA2), The Second Southern Sky Redshift Survey (SSRS2), The DEEP2 Redshift Survey (DEEP2), Two-Degree Field Redshift Survey (2dF)] and information about the radial velocities of galaxies, the application of 3D methods of selection became generally accepted. 3D methods of group identification use as a rule two limited parameters: projected distance between galaxies R and radial velocity difference ΔV . For example, Barton, Geller & Kenyon (2000, 2003), Geller et al. (2006) and Woods, Geller & Barton (2006) selected close pairs of galaxies from the CfA2 catalogue with $R < 50$ kpc and $\Delta V < 1000 \text{ km s}^{-1}$; the isolation criterion was ignored. Patton et al. (2000) investigated galaxy pairs from SSRS2. They considered all pairs with $R < 100$ kpc and did not find pairs with signs of interaction with $\Delta V > 600 \text{ km s}^{-1}$, but most pairs with interaction signs had $R < 20$ kpc and $\Delta V < 500 \text{ km s}^{-1}$ (see also Patton et al. 2002; Xu, Sun & He 2004; Patton, Grant & Simard 2005; De Propriis et al. 2007). Nikolic, Cullen & Alexander (2004) obtained similar results for SDSS pairs. The authors found that the star formation rate is significantly enhanced for projected separations less than 30 kpc. Lambas et al. (2003) and Alonso et al. (2004) considered galaxy pairs with $R < 1$ Mpc and $\Delta V < 1000 \text{ km s}^{-1}$ from the 2dF survey. They analysed the star formation activity in the pairs as a function of both relative projected distance and relative radial velocity, and found that the star formation activity in galaxy pairs is significantly enhanced over that in isolated galaxies at similar redshifts for $R < 25$ kpc and $\Delta V < 100 \text{ km s}^{-1}$. Soares (2007) showed that more than half of the simulated pairs with projected distance $R \leq 50$ kpc have 3D separations greater than 50 kpc. Therefore for the selection of real physical pairs, it is important to take into account the signs of interaction, but that is not always possible.

Triplets of galaxies are less studied than pairs. Mainly triplets have been selected from the catalogues of groups of different populations (Trofimov & Chernin 1995). For example, Karachentseva et al. (2005), Vavilova et al. (2005), Melnyk (2006) and Melnyk & Vavilova (2006) compared the kinematic, dynamical, configurational and morphological properties of triplets from samples formed by the different methods. They showed that physical properties of galaxy groups strongly depend on selection criteria.

The main goal of our paper is to provide the uniform selection of single galaxies, pairs and triplets from SDSS¹ for later analysis of their properties: mass-to-luminosity ratio, colour indices, morphology and others. Such an investigation can be helpful for the study of the environmental influence and dark matter content on small scales (galaxy – pair – triplet). To meet this goal, we made selection of not only the most isolated galaxies and systems, but also single galaxies, pairs and triplets with different isolation degrees.

Most authors mentioned above used simple selection algorithms for pair identification: they consider all pairs with the fixed limitation parameters R and ΔV , which describe properties of the galaxy

pair only as a separate system, without information about their neighbours. Contrary to this, we propose another approach. We use the second-order Voronoi tessellation for galaxy pair identification where the fundamental elements are pairs, and the third-order Voronoi tessellation for galaxy triplet identification where the fundamental elements are triplets. The geometric properties of the high-order tessellations give information about the relative location of neighbouring galaxies. This allows us to analyse the correlations of group properties with environment. The high-order (second- or third-order) Voronoi tessellation method has not been applied earlier for group detection, unlike the first-order Voronoi tessellation. Using the galaxies from the SDSS DR5 survey with known redshifts allows us to realize the 3D approach.

The outline of the paper is as follows. In Section 2, we present the method and parameters. The sample of galaxies is described in Section 3. In Section 4, we discuss our results and compare them with other works. Our conclusions are presented in Section 5.

2 THE METHOD AND PARAMETERS

The Voronoi diagram was introduced by Voronoi (1908). The most popular is the first-order Voronoi diagram (so-called Voronoi tessellation), Fig. 1(a). It is a geometric method of space partition on regions. Each region consists of one nucleus and all the points of space that are closer to a given nucleus than to other nuclei (Matsuda & Shima 1984; Lindenbergh 2002). Kiang (1966) found an analytic function of the Voronoi cell volume distribution for random points in 2D and 3D space. The Voronoi tessellation is used widely in astrophysics, especially for modelling the galaxy and void large-scale structure distribution (Icke & van de Weygaert 1987; van de Weygaert & Icke 1989; van de Weygaert 1994; Zaninetti 2006; van de Weygaert & Schaap 2007), for studying periodicities in deep pencil-beam sky surveys (Ikeuchi & Turner 1991; van de Weygaert 1991; Williams, Peacock & Heavens 1991; SubbaRao & Szalay 1992; Gonzales et al. 2000), for the extragalactic radio source distribution (Benn & Wall 1995) and for modelling of the cosmic microwave background anisotropy (Coles & Barrow 1990; SubbaRao et al. 1994) etc. Ebeling & Wiedenmann (1993) were the first to apply the Voronoi tessellation for finding groups and clusters of galaxies in the 2D case. Later such an approach was used by Ramella et al. (2001), Kim et al. (2002), Lopes et al. (2004), Barrena et al. (2005) and Panko & Flin (2006). The 3D Voronoi tessellation for galaxy group identification was realized by Marinoni et al. (2002) and Cooper et al. (2005). The application of the 3D Voronoi tessellation to the DEEP2 survey was introduced by Gerke et al. (2005). Melnyk, Elyiv & Vavilova (2006) applied the first-order 3D Voronoi tessellation for the identification of galaxy groups in the local supercluster. The authors demonstrated that the first-order tessellation is more useful for searching the rich clusters of galaxies than the small groups. In the first-order Voronoi tessellation, the key parameter is the volume of the galaxy's Voronoi cell V . This parameter characterizes a galaxy environmental density. The condition of cluster/group membership of a certain galaxy is the relatively small value of V . This condition is true when the galaxy is surrounded by close neighbouring galaxies. That is why the first-order Voronoi tessellation is not corrected for the identification of small isolated galaxy systems (see Melnyk et al. 2006 for details). In this paper, we propose the high-order 3D Voronoi tessellation method for identification of pairs and triplets. Let us consider this method below.

Contrary to the first-order tessellation (Fig. 1a), the second-order tessellation for set S distribution of nuclei is the partition of the

¹ <http://www.sdss.org>

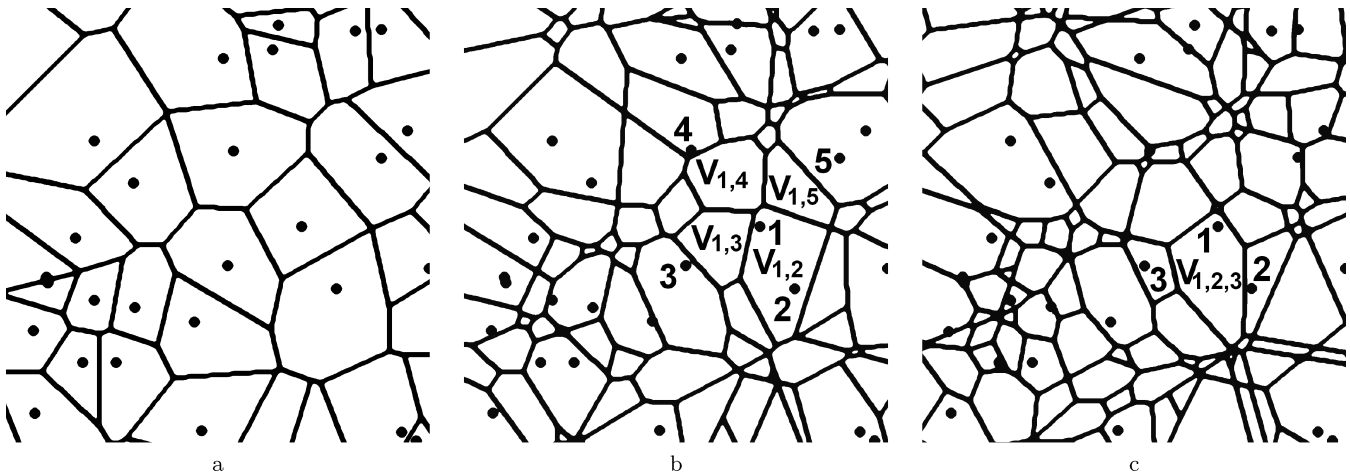


Figure 1. 2D Voronoi tessellation of the first (a), second (b) and third (c) order for the same distribution of random nuclei.

space which associates a region $V_{1,2}$ with each pair of nuclei 1 and 2 from S in such a way that all points in $V_{1,2}$ are closer to 1 and 2 than other nuclei from S (Fig. 1b). Region $V_{1,2}$ is a *common cell* for nuclei 1 and 2.² In such a way, the second-order Voronoi tessellation is available for the identification of single galaxies and pairs.

The third-order Voronoi tessellation is appropriate for the identification of triplets. It is the partition of the space which associates a region $V_{1,2,3}$ with each triplet of nuclei 1, 2, 3 in such a way that all points in $V_{1,2,3}$ are closer to nuclei 1, 2, 3 than other nuclei from S (Lindenbergh 2002), Fig. 1(c).

Since we work with a sample of galaxies, we use galaxies as the nuclei of the Voronoi tessellation taking into account equatorial coordinates α , δ and radial velocities of galaxies V_h only. For the construction of the 3D Voronoi tessellations, it is necessary to determine the distances in 3D space. The spatial distance between two galaxies can be decomposed into projected (tangential) distance r and radial component v (difference of the radial velocities). We can determine the projected distance with a relatively high accuracy, while the radial component has errors owing to inaccuracy of radial velocity measurement of each galaxy and existing strong peculiar velocities (due to virial motions of galaxies in groups and clusters). As a result the galaxy distribution in space of radial velocities is extended along the radial component, the so-called fingers-of-God effect. This is attributed to the random velocity dispersions in a galaxy volume-limited sample that cause a galaxy's velocity to deviate from pure Hubble flow, stretching out a group of galaxies in redshift space (Jackson 1972). Various authors take into account this effect in their own way depending on the specifics of their problem. For example, Marinoni et al. (2002) chose some cylindrical window of clustering which is extended along the radial component. We propose a different way that is based on introduction of weight for a radial component (see Appendix A). Such an approach allows us to avoid the problem of tangential and radial distance inequivalence and to apply the high-order 3D Voronoi tessellation method.

² However, it is not necessary that these nuclei lie in the common cell. For example, nuclei 1 and 5 create the common cell $V_{1,5}$ and they do not lie in this cell.

2.1 Second-order Voronoi tessellation: pairs and single galaxies

The second-order Voronoi tessellation was applied for the identification of pairs and single galaxies in the following way. Each galaxy i from set S forms common cells with a certain number of neighbouring galaxies (Fig. 1b). So we define the *neighbouring galaxies* of galaxy i as only galaxies that create common cells with this galaxy. For example, galaxy 1 creates only four common cells ($V_{1,2}$, $V_{1,3}$, $V_{1,4}$, $V_{1,5}$) with neighbouring galaxies 2, 3, 4 and 5, respectively. Each pair of galaxies i, j is characterized by the dimensionless parameters $p_{i,j}$:

$$p_{i,j} = \frac{D\sqrt{V_{i,j}}}{m_{i,j}}, \quad (1)$$

where D is the space dimension, $V_{i,j}$ is the area (for 2D) or volume (for 3D) of the cell, and $m_{i,j}$ is the distance between galaxies i and j (see Appendix A).

Each galaxy has a set of $p_{i,j}$ parameters. For example, galaxy 1 has the set $p_{1,2}, p_{1,3}, p_{1,4}, p_{1,5}$. We choose the maximum value from the set of parameters for galaxy 1: $p_{\max}(1) = \max(p_{1,2}, p_{1,3}, p_{1,4}, p_{1,5})$. In the general case for galaxy i : $p_{\max}(i) = \max(p_{i,j})$, where j assumes numbers of k neighbours.

We define the *geometric pair* in the second-order Voronoi tessellation as such a pair which contains two galaxies with a common cell that have the same p_{\max} parameters, $p_{\max}(1) = p_{\max}(2) = p$. The parameter p characterizes a *degree of geometric pair isolation*. By a degree of pair isolation, we mean the overdensity relative to the background. We used the principle which was applied by Karachentsev (1987) for the selection of isolated galaxy pairs: if all galaxies have the same angular diameter, a neighbour of a pair of galaxies should be located on the sky more than five times farther from a pair than the separation of the pair members from each other. In our 3D approach, the degree of pair isolation is described by the relation between volume $V_{1,2}$ of the common cell (it characterizes distance to neighbours) and the distance $m_{1,2}$ between pair members according to equation (1). For example, a strongly isolated pair has a large value of p due to a large $V_{1,2}$ and small $m_{1,2}$ (1), see also Fig. 2(a).

We also introduce the parameter p_e which describes only the *pair environment* and does not depend on distance between pair members directly. We define it as the mean value of the $p_j(1)$ and

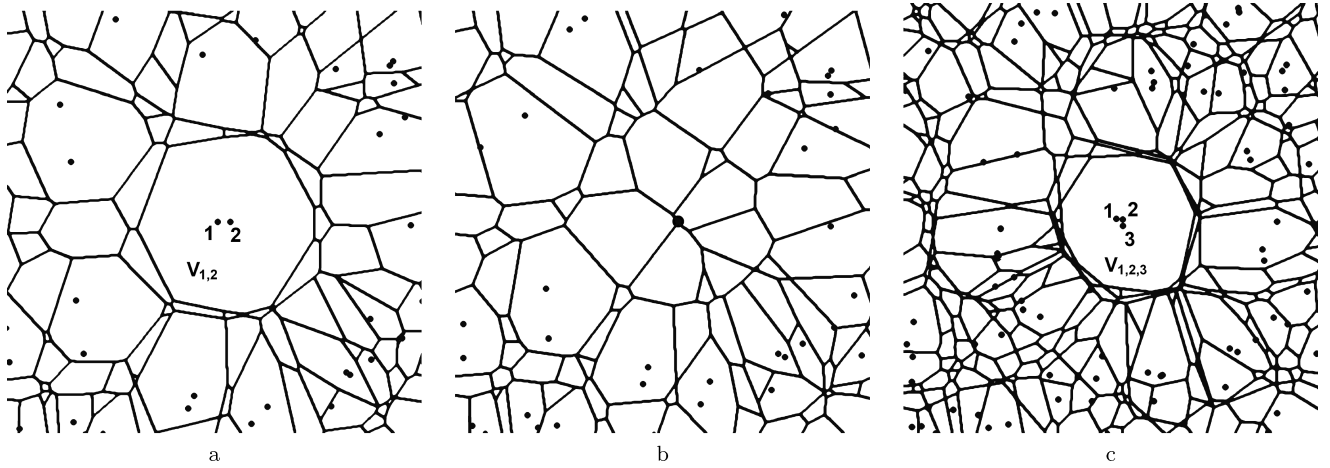


Figure 2. Different configurations of the galaxies: isolated close pair (a) and isolated single galaxy (b) in the second-order tessellation, and isolated close triplet in the third-order tessellation (c).

$p_l(2)$ parameters of the first and second galaxy, excepting p from both sets:

$$p_e = \frac{\sum_{j=2}^k p_j(1) + \sum_{l=2}^n p_l(2)}{k + n - 2}, \quad (2)$$

where k and n are the numbers of neighbouring galaxies for 1 and 2 galaxies of the geometric pair, respectively. We start the sums from $j = 2$ and $l = 2$ for excepting $2p$, because the first galaxy is a neighbour of the second galaxy and vice versa. Therefore, $k + n - 2$ is the sum of neighbouring galaxies of pair members excepting pair galaxies as being neighbours for each other. Parameter p_e depends on the distribution of neighbouring galaxies. A small value of p_e points out that such a pair is located in a loose environment. In such a case, the average volume of common cells of pair components with neighbouring galaxies is relatively small, and distance between them is large, see formula (1) and Fig. 2(a).

A *single galaxy* is a galaxy which is not a member of any geometric pair. The single galaxies are field galaxies in the environment of geometric pairs. Every single galaxy has its own neighbours; single galaxies and geometric pair members can be among them. According to the second-order Voronoi tessellation, the larger the degree of galaxy isolation, the greater is the number of neighbours (see Fig. 1b in comparison with Fig. 2b), but these neighbours are located farther away. The best parameter that describes the isolation degree of a single galaxy is the mean value of all parameters p_j of this galaxy:

$$s = \frac{\sum_{j=1}^k p_j}{k}, \quad (3)$$

where k is the number of neighbours. Therefore, the smaller the value of s , the more isolated is the single galaxy.

2.2 Third-order Voronoi tessellation: triplets

The method of the third-order Voronoi tessellation can be introduced in the same way as the second-order approach (Fig. 1c). All points of the common triplet's cell are closer to galaxies of this triplet than to other galaxies. Similarly to the parameter $p_{i,j}$ for pairs, we set up the parameter $t_{i,j,u}$ for triplets:

$$t_{i,j,u} = \frac{D \sqrt{V_{i,j,u}}}{\max(m_{i,j}, m_{i,u}, m_{j,u})}, \quad (4)$$

where D is the space dimension, $V_{i,j,u}$ is the area (for 2D) or volume (for 3D) of the cell, and $m_{i,j}$, $m_{i,u}$, $m_{j,u}$ are the distances between galaxies in the triplet.

A *geometric triplet* in the third-order Voronoi tessellation contains three galaxies that have a common cell and the same maximal parameters $t_{\max}(1) = t_{\max}(2) = t_{\max}(3) = t$. The parameter t characterizes a *degree of geometric triplet isolation*. We define the parameter of *triplet environment* t_e as the mean value of parameters $t_i(1)$, $t_j(2)$ and $t_u(3)$, except t from three sets:

$$t_e = \frac{\sum_{i=2}^k t_i(1) + \sum_{j=2}^n t_j(2) + \sum_{u=2}^q t_u(3)}{k + n + q - 3}; \quad (5)$$

here in the case of the third-order Voronoi tessellation, k , n and q denote the number of *neighbouring triplets* which contain galaxies 1, 2 and 3, respectively. Therefore, $k + n + q - 3$ is the number of neighbouring triplets for a certain triplet that contain at least one galaxy from this triplet.

It can be seen from Fig. 2(c) and equations (4) and (5) that for the triplet with the highest degree of standing out against a background, the isolation parameter t has the highest value. At the same time, if the triplet neighbours are located far from it, parameter t_e has a small value.

Parameters p , s , t are the basic ones and define the isolation degree of a galaxy pair, single galaxy or triplet in comparison with the background, respectively. Parameters p_e and t_e are additional ones and contain information about the distribution of the neighbouring galaxies (environment).

Similarly to the second- and third-order Voronoi tessellations, it is possible to apply more high-order Voronoi tessellations for the identification of galaxy quartets, quintets and so on.

3 THE SAMPLE

For our investigation, we used the Northern part of the SDSS DR5 spectroscopic survey. Our sample is volume limited and consists of objects that are classified as galaxies. The primary sample had contained approximately 11 000 galaxies with radial velocities from 2500 to 10 000 km s⁻¹, $H_0 = 75$ km s⁻¹ Mpc⁻¹. It is known that the completeness of the SDSS is poor for the bright galaxies because of spectroscopic selection criteria and the difficulty of obtaining correct photometry for objects with large angular size. We tried to

decrease the influence of this effect due to limiting of our sample $V_h > 2500 \text{ km s}^{-1}$, i.e. so as not to take into account nearest objects with large angular diameter. Such a volume limiting also helps us to avoid influence of the Virgo cluster where strong peculiar motion exists. We checked additionally all pairs of galaxies with a small angular resolution and excluded identical objects (parts of galaxies), which are presented twice and more in the SDSS survey. All galaxy velocities V_h were corrected for the Local Group centroid V_{LG} according to Karachentsev & Makarov (1996). When we had applied the high-order Voronoi tessellation method to the SDSS catalogue, we limited our sample to $3000 \leq V_{LG} \leq 9500 \text{ km s}^{-1}$. We did not consider also galaxies that are located within 2° near borders, because the correct estimation of the Voronoi cell volume is not possible in this case. Our volume-limited sample is complete up to 17.7 mag but contains also about 100 more fainter galaxies. The final number of galaxies in the sample is 6786.

4 THE RESULTS

We applied the second-order 3D Voronoi tessellation to our sample of 6786 galaxies and obtained 2196 geometric pairs and 2394 single galaxies (65 per cent galaxies of whole sample are in pairs and 35 per cent are singles). We divided our samples of geometric pairs and singles into four equal parts by the parameters of isolation p and s , respectively. A quarter of each sample with the highest isolation degree we called *isolated* (549 pairs and 598 singles). It means that the isolated pairs and singles have $p > Q_3$ and $s < Q_1$, respectively; Q_3 is the third quartile and Q_1 is the first quartile. See values of quartiles in Table 1.

Fig. 3 shows the distributions of number of neighbouring galaxies for galaxies that are members of pairs and singles. We can see from Fig. 3 that number of neighbours is varied through the range from 4 to 30 galaxies. Isolated galaxies have more neighbours than

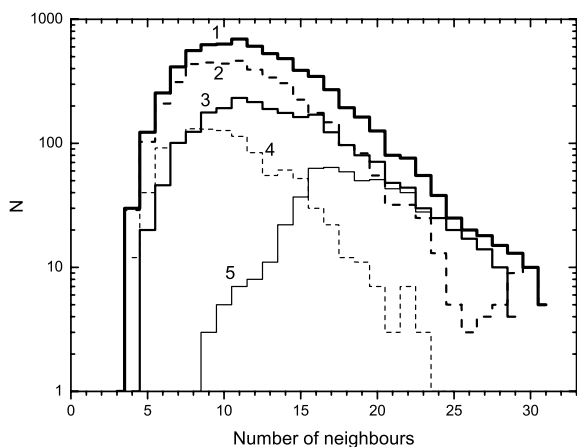


Figure 3. Distributions of number of neighbouring galaxies: (1) all galaxies of the sample, (2) galaxies in geometric pairs, (3) single galaxies, (4) galaxies in isolated pairs and (5) isolated galaxies.

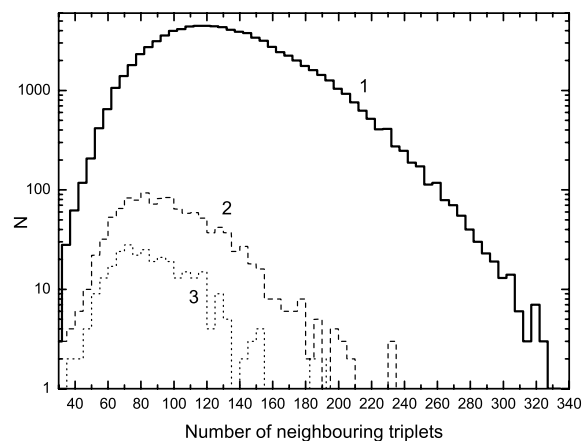


Figure 4. Distributions of number of neighbouring triplets: (1) all triplets of the sample, (2) geometric triplets and (3) isolated triplets.

galaxies in other samples on average. It is a feature of the second-order Voronoi tessellation (see above). Galaxies in isolated pairs have approximately half as many neighbours as isolated galaxies because the pair's neighbours distribute between two members.

Independently, we applied the third-order 3D Voronoi tessellation to our galaxy sample and obtained 1182 geometric triplets (52 per cent of the whole sample). The quarter (297) of the triplet sample with the highest isolation degree $t > Q_3$ we called *isolated*. Values of all quartiles for triplets can be found in Table 1. The distribution of numbers of neighbouring triplets is shown in Fig. 4. As can be seen, this picture looks the same as for the distribution of number of neighbouring galaxies in the case of the second-order Voronoi tessellation (Fig. 3).

4.1 Comparison with other samples

We cross-correlated our results with other samples. To first order, we compared pairs and triplets of our sample with Tago et al. (2008) groups selected by the modified friends-of-friends method using the same release of SDSS. From 965 galaxies of Tago's pairs that are located in our region of investigation, 686 galaxies (343 pairs or 71 per cent) coincide with our pairs with different isolation degree. The median value of the isolation parameter p is 9.89 which does not differ strongly from our isolation limit ($Q_3 = 10.17$). Another 121 galaxies coincide with one of our pair members; the median value of p for these pairs is 3.94. We can conclude that they are located in the field. The remaining 158 galaxies coincide with our single galaxies having isolation degree $s = 0.87$, i.e. also associated with the field galaxies (our isolation limit is less than $Q_1 = 0.57$). 63 triplets (51 per cent) of the Tago et al. (2008) triplets that fall in our region coincide with our triplets. The median value of isolation degree for these triplets $t = 4.83$ is higher than our isolation limit $Q_3 = 3.90$. We also compared our pairs with 28 isolated Karachentsev (1987) pairs that are located in our region of investigation: 16 pairs coincide with our pairs (the median value of isolation degree $p = 21.16$ is very high). Among seven of our 'pairs', one of the components is an interacting galaxy which corresponds to Karachentsev's pair, the second component is a fainter galaxy, these 'pairs' are not isolated (median value of p is 3.95). Such cases appear because of difficulties in the spectroscopic measurement of interacting (very close) galaxies in the SDSS. The remaining five pairs coincide by components with different pairs and single galaxies with small isolation degree because these pairs are surrounded by fainter satellites. We found

that 10 out of 36 KIG galaxies coincided with our single galaxies, but 24 KIG galaxies fall in our pairs with different isolation degree (the median value is not very high, $p = 5.8$). Such a difference can be explained by the presence of a fainter galaxy in the immediate vicinity of the KIG galaxy. Actually, all 34 isolated galaxies with fainter satellites from Prada et al. (2003), which locate in our region, coincide with our pairs and triplets.

We can conclude that our singles, pairs and triplets of galaxies obtained by the high-order Voronoi tessellation are in good agreement with other samples, especially concerning the systems with high isolation degrees. Some lack of coincidence can be explained by the differences in primary catalogues, for example, by the magnitude depth or spectroscopy of interacting galaxies in the SDSS.

4.2 Isolation and main parameters

In addition to the isolation and environmental parameters p , p_e , s , t and t_e , we calculated also other characteristics (Karachentsev, Karachentseva & Lebedev 1989; Vavilova et al. 2005): rms velocity of galaxies with respect to the group centre (in km s^{-1}), $S_v = [\frac{1}{N} \sum_{k=1}^N (V_{LG}^k - \langle V_{LG} \rangle)^2]^{1/2}$, $S_v = \Delta V/2$ for pairs, N is the number of galaxies in the group; harmonic mean radii of the system (in kpc) – $R_h = (\frac{1}{3} \sum_{i,k} R_{ik}^{-1})^{-1}$, where $R_{ik} = X_{ik} \langle V_{LG} \rangle H_0^{-1}$ and X_{ik} is the relative angular distance; R is the maximal distance between galaxies in triplets, for galaxy pair $R_h = R$; dimensionless crossing-time

$$\tau = 2H_0 R_h / S_v \quad (6)$$

expressed in units of the cosmological time H_0^{-1} ; virial mass

$$M_{\text{vir}} = 3\pi N(N-1)^{-1} G^{-1} S_v^2 R_h \quad (7)$$

in M_\odot ; galaxy luminosity L_r , which corresponds to the Petrosian magnitude in the r band, L_\odot ; and mass-to-luminosity ratio $M_{\text{vir}}/L = M_{\text{vir}} / \sum L_r$ in M_\odot/L_\odot .

First of all we investigated how the values of rms velocity and mean harmonic radius of pairs and triplets depend on their isolation degree. Table 2 presents the median values and quartiles of S_v and R_h for pairs and triplets in dependence on isolation parameters p and t : all geometric pairs, pairs with $p > Q_1$, $p > Q_2$, $p > Q_3$; all geometric triplets, triplets with $t > Q_1$, $t > Q_2$, $t > Q_3$, where Q_1 , Q_2 , Q_3 is the first, second (median value), third quartile, respectively. See values of p and t quartiles in Table 1. It can be seen from Table 2 that all geometric samples have largest values of S_v and R_h and largest interquartile range (IQR). With the increase in isolation degree, the

medians and IQR of S_v and R_h decrease. Pairs and triplets selected by a dynamical method (Makarov & Karachentsev 2000) have medians $S_v = 24_{-13}^{+22} \text{ km s}^{-1}$, $R_h = 170_{-114}^{+185} \text{ kpc}$ and $41_{-18}^{+19} \text{ km s}^{-1}$, $191_{-88}^{+157} \text{ kpc}$, respectively. The sample of triplets from Vavilova et al. (2005) has medians $S_v = 30_{-12}^{+18} \text{ km s}^{-1}$ and $R_h = 160_{-77}^{+117} \text{ kpc}$. These values better agree with samples which have $p, t > Q_2$ (i.e. $p > 5.72$ and $t > 2.62$ for pairs and triplets, respectively).

We also considered how the isolation degree of pairs and triplets depends on S_v and R_h . Tables 3 and 4 give values of parameters p , p_e , t , t_e for pairs and triplets at the fixed values of S_v and R_h , which correspond to intervals: $S_v, R_h < Q_1$; $Q_1 < S_v, R_h < Q_2$; $Q_2 < S_v, R_h < Q_3$; $S_v, R_h > Q_3$; All S_v, R_h .

Most compact pairs with R_h less than the first quartile have medians of p 2.5 times greater and IQR almost three times greater than the values for sample ‘All S_v, R_h ’. This means that compact pairs are more isolated (or higher contrast in comparison with the background) than in average galaxies in the whole sample, but also they are characterized by different isolation degree. At $R_h < Q_1$ and $p, t > Q_3$, 65 per cent of pairs (47 per cent of triplets) coincide.

Parameter p_e for the compact pairs has a large dispersion also. This means that similar compact pairs are in both densest and loose environments. Thus, the isolation degree and IQR change depending on the values of rms velocities: the most compact pairs with rms velocity less than the first quartile are most isolated. For these pairs, parameter p is almost five times greater than the median of the ‘All R_h, S_v ’ sample and IQR is 4.5 times greater. Most compact pairs with $S_v > Q_3$ have an isolation degree the same as galaxies of the whole sample. The values of isolation parameter decrease with increasing of R_h and S_v , thus, at R_h greater than third quartile the p becomes almost two times less than the median of the whole sample. It means that these pairs are less isolated. It is necessary to note that p significantly changes in dependence on R_h , compared with S_v . But all of the pairs with $S_v > 40 \text{ km s}^{-1}$ (Q_3) are characterized by small isolation degree, compared with pairs with $S_v < 40 \text{ km s}^{-1}$. The additional parameter p_e also decreases with R_h increasing and for $R_h > Q_3$ it has the minimum value with a small variation (p is also minimal). So, all wide pairs ($R_h > Q_2$) are in low-density environments. It is obvious that there is not enough free space for the widest pairs to be isolated (without galaxies). Most probably, these pairs are the accidental ones in the common field. From Table 4, it is easy to be convinced that all of the above-mentioned tendencies are similar for triplets but with their own values.

4.3 The luminosity content

Considering the luminosity–density relation (e.g. Park et al. 2007, 2008, and references therein), we can note the following: galaxies are more luminous in the high-density regions than in the field. Karachentseva et al. (2005) showed that galaxies even in such poor groups as the triplets are more luminous than the isolated galaxies. We compared the luminosities of single/isolated galaxies with the luminosities of galaxies in pairs and triplets. Their medians with quartiles and mean values with standard deviations are presented in Table 5. Fig. 5 shows the distribution of galaxy luminosities.

It can be seen from Table 5 and Fig. 5 that the median and mean values of luminosities are greater for galaxies in pairs and triplets than for single/isolated galaxies. The mean values of luminosities of isolated galaxies and galaxies in isolated pairs differ significantly (with a probability of >0.99 by the t -criterion), but differences for ‘All’ samples are not statistically significant. The same conclusions

Table 2. Physical properties of pairs and triplets: dependence on isolation parameters.

| Pairs | N | S_v | R_h |
|---------------|------|------------------|---------------------|
| Pairs | | | |
| All geometric | 2196 | 22_{-11}^{+18} | 354_{-199}^{+336} |
| $p > Q_1$ | 1677 | 20_{-11}^{+15} | 252_{-130}^{+217} |
| $p > Q_2$ | 1038 | 18_{-10}^{+12} | 182_{-91}^{+156} |
| $p > Q_3$ | 549 | 16_{-8}^{+8} | 106_{-47}^{+73} |
| Triplets | | | |
| All geometric | 1182 | 41_{-15}^{+20} | 390_{-184}^{+333} |
| $t > Q_1$ | 893 | 38_{-14}^{+16} | 330_{-148}^{+216} |
| $t > Q_2$ | 582 | 35_{-12}^{+14} | 275_{-109}^{+194} |
| $t > Q_3$ | 297 | 31_{-10}^{+11} | 212_{-83}^{+132} |

Table 3. Parameters p and p_e at fixed values S_v and R_h for geometric pairs.

| Pairs | | $S_v < 10$ | $10 < S_v < 22$ | $22 < S_v < 40$ | $S_v > 40$ | All S_v |
|----------------------|-------|---------------------------|--------------------------|-------------------------|------------------------|--------------------------|
| $R_h < 155$ | p | $27.61^{+17.57}_{-12.68}$ | $18.90^{+13.44}_{-6.65}$ | $11.84^{+5.62}_{-3.88}$ | $6.14^{+2.91}_{-1.38}$ | $14.67^{+13.09}_{-5.93}$ |
| | p_e | $0.90^{+0.38}_{-0.20}$ | $0.94^{+0.55}_{-0.30}$ | $0.87^{+0.38}_{-0.24}$ | $0.63^{+0.19}_{-0.14}$ | $0.85^{+0.37}_{-0.24}$ |
| | N | 149 | 153 | 144 | 103 | 549 |
| $155 \leq R_h < 354$ | p | $8.85^{+3.37}_{-2.74}$ | $8.47^{+4.72}_{-2.49}$ | $7.05^{+2.57}_{-2.18}$ | $4.87^{+1.71}_{-1.10}$ | $7.36^{+3.18}_{-2.31}$ |
| | p_e | $0.83^{+0.25}_{-0.18}$ | $0.83^{+0.32}_{-0.20}$ | $0.82^{+0.19}_{-0.18}$ | $0.66^{+0.14}_{-0.12}$ | $0.78^{+0.23}_{-0.18}$ |
| | N | 146 | 154 | 133 | 116 | 549 |
| $354 \leq R_h < 690$ | p | $5.45^{+1.65}_{-1.43}$ | $5.23^{+2.34}_{-1.39}$ | $4.73^{+1.79}_{-1.18}$ | $4.03^{+1.31}_{-0.93}$ | $4.84^{+1.84}_{-1.21}$ |
| | p_e | $0.64^{+0.17}_{-0.13}$ | $0.63^{+0.18}_{-0.10}$ | $0.69^{+0.14}_{-0.12}$ | $0.59^{+0.15}_{-0.13}$ | $0.64^{+0.15}_{-0.13}$ |
| | N | 153 | 130 | 139 | 127 | 549 |
| $R_h \geq 690$ | p | $3.12^{+1.32}_{-0.82}$ | $3.27^{+1.21}_{-0.81}$ | $3.05^{+1.17}_{-0.70}$ | $2.42^{+0.90}_{-0.43}$ | $2.83^{+1.10}_{-0.65}$ |
| | p_e | $0.47^{+0.11}_{-0.09}$ | $0.46^{+0.09}_{-0.09}$ | $0.52^{+0.07}_{-0.10}$ | $0.47^{+0.10}_{-0.08}$ | $0.48^{+0.10}_{-0.09}$ |
| | N | 101 | 112 | 133 | 203 | 549 |
| All R_h | p | $7.27^{+6.74}_{-2.78}$ | $7.57^{+6.47}_{-3.32}$ | $5.63^{+3.77}_{-1.94}$ | $3.81^{+1.92}_{-1.24}$ | $5.72^{+4.45}_{-2.13}$ |
| | p_e | $0.71^{+0.25}_{-0.20}$ | $0.70^{+0.29}_{-0.19}$ | $0.69^{+0.26}_{-0.16}$ | $0.55^{+0.15}_{-0.12}$ | $0.65^{+0.24}_{-0.15}$ |
| | N | 549 | 549 | 549 | 549 | 2196 |

Table 4. Parameters t and t_e at fixed values S_v and R_h for geometric triplets.

| Triplets | | $S_v < 26$ | $26 < S_v < 41$ | $41 < S_v < 61$ | $S_v > 61$ | All S_v |
|----------------------|-------|------------------------|------------------------|------------------------|------------------------|------------------------|
| $R_h < 205$ | t | $5.22^{+2.24}_{-2.12}$ | $4.33^{+2.84}_{-1.42}$ | $3.47^{+1.40}_{-1.11}$ | $2.25^{+0.71}_{-0.29}$ | $3.75^{+2.53}_{-1.23}$ |
| | t_e | $0.43^{+0.14}_{-0.08}$ | $0.41^{+0.09}_{-0.06}$ | $0.36^{+0.05}_{-0.06}$ | $0.29^{+0.05}_{-0.05}$ | $0.38^{+0.10}_{-0.07}$ |
| | N | 91 | 92 | 70 | 43 | 296 |
| $205 \leq R_h < 390$ | t | $3.44^{+1.74}_{-0.82}$ | $3.36^{+1.13}_{-1.04}$ | $2.84^{+1.05}_{-1.64}$ | $2.25^{+0.69}_{-0.29}$ | $3.11^{+1.17}_{-0.85}$ |
| | t_e | $0.41^{+0.05}_{-0.07}$ | $0.38^{+0.05}_{-0.07}$ | $0.37^{+0.04}_{-0.06}$ | $0.32^{+0.03}_{-0.04}$ | $0.37^{+0.06}_{-0.06}$ |
| | N | 81 | 87 | 83 | 44 | 295 |
| $390 \leq R_h < 723$ | t | $2.96^{+0.83}_{-0.78}$ | $2.47^{+0.92}_{-0.57}$ | $2.50^{+0.74}_{-0.47}$ | $2.03^{+0.38}_{-0.44}$ | $2.42^{+0.79}_{-0.54}$ |
| | t_e | $0.31^{+0.09}_{-0.04}$ | $0.32^{+0.05}_{-0.04}$ | $0.33^{+0.06}_{-0.04}$ | $0.29^{+0.05}_{-0.03}$ | $0.32^{+0.06}_{-0.05}$ |
| | N | 71 | 65 | 76 | 83 | 295 |
| $R_h \geq 723$ | t | $1.92^{+0.92}_{-0.36}$ | $1.97^{+0.33}_{-0.25}$ | $1.89^{+0.61}_{-0.35}$ | $1.74^{+0.69}_{-0.31}$ | $1.88^{+0.64}_{-0.38}$ |
| | t_e | $0.25^{+0.04}_{-0.05}$ | $0.27^{+0.03}_{-0.05}$ | $0.27^{+0.04}_{-0.04}$ | $0.24^{+0.02}_{-0.03}$ | $0.25^{+0.03}_{-0.04}$ |
| | N | 53 | 51 | 66 | 126 | 296 |
| All R_h | t | $3.23^{+1.96}_{-0.97}$ | $3.08^{+1.37}_{-1.01}$ | $2.65^{+1.02}_{-0.65}$ | $2.03^{+0.57}_{-0.44}$ | $2.62^{+1.28}_{-0.71}$ |
| | t_e | $0.37^{+0.09}_{-0.09}$ | $0.35^{+0.08}_{-0.07}$ | $0.33^{+0.07}_{-0.05}$ | $0.27^{+0.05}_{-0.04}$ | $0.32^{+0.07}_{-0.06}$ |
| | N | 296 | 295 | 295 | 296 | 1182 |

Table 5. Comparison between the luminosities of the galaxies from different samples.

| Sample of galaxies | $L_r \times 10^9 (L_\odot)$ | |
|------------------------|-----------------------------|-------------|
| | Median | Mean (SD) |
| All single | $2.23^{+3.66}_{-1.15}$ | 5.17 (8.00) |
| All geometric pairs | $2.38^{+4.27}_{-1.29}$ | 5.79 (8.66) |
| All geometric triplets | $2.48^{+1.36}_{-0.14}$ | 6.00 (8.77) |
| Isolated | $1.80^{+3.10}_{-0.77}$ | 3.52 (4.47) |
| Isolated pairs | $2.89^{+7.20}_{-1.73}$ | 6.74 (9.46) |
| Isolated triplets | $2.68^{+6.80}_{-1.52}$ | 6.53 (9.97) |

can be drawn from the comparison of the sample of single/isolated galaxies with galaxies in triplets.

So, galaxies in isolated pairs and triplets are two times more luminous than isolated galaxies. It is necessary to note that our

method of group identification does not take into account individual physical characteristics of galaxies, therefore the effects of selection are absent here. The fact that for ‘All’ samples the mean values have a small difference may serve as evidence of the influence of non-physical (accidental) groups in these samples; the wide systems are dominant among them.

4.4 Mass-to-luminosity ratio

For studying the presence and distribution of dark matter in small galaxy groups, we used the mass-to-luminosity ratio (M_{vir}/L) as the quantitative indicator of dark matter contribution. We checked the mass-to-luminosity ratio in dependence on the isolation degree of pairs and triplets. We plotted the dependences of system isolation p , t on M_{vir}/L in narrow bins of R , because the isolation parameters p , t and virial mass M_{vir} depend on the projected distance between the galaxies R (see equations 1, 4 and 7). Fig. 6 presents the dependence of slope α in the p , t - M_{vir}/L relation on R , and Fig. 7 presents

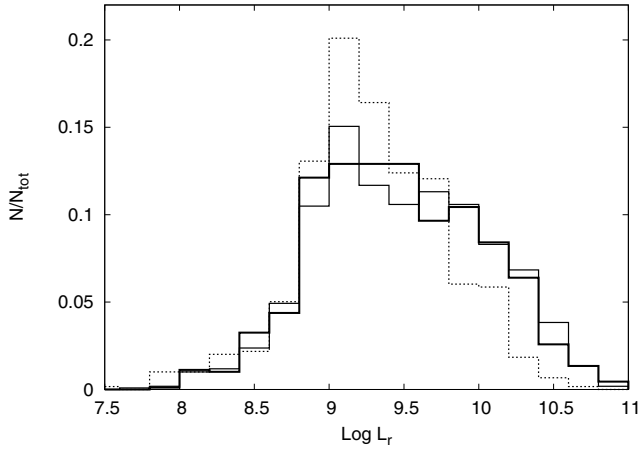


Figure 5. Luminosity distributions of isolated galaxies (dotted line), galaxies in isolated pairs (solid line) and galaxies in isolated triplets (thick line).

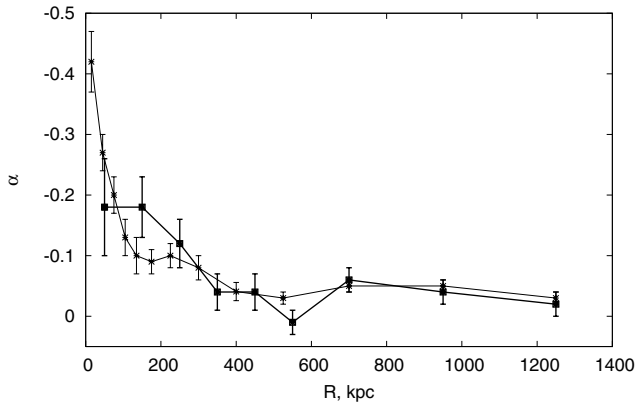


Figure 6. Dependence between slope α and R : for the pairs $\log(p) = \alpha \log(M_{\text{vir}}/L) + b$ (thin line) and for the triplets $\log(t) = \alpha \log(M_{\text{vir}}/L) + b$ (thick line).

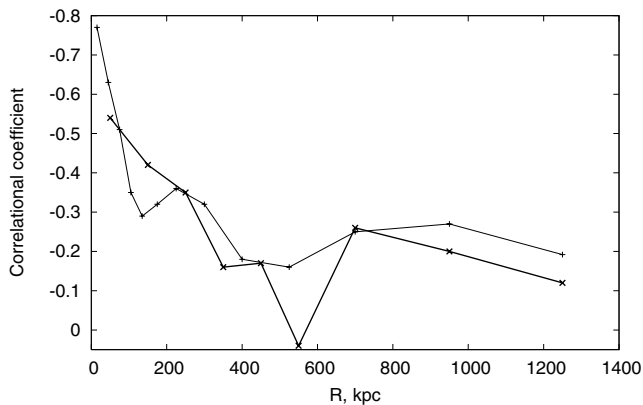


Figure 7. Dependence of correlation coefficient in relations from Fig. 6 on R : for the pairs (thin line) and for the triplets (thick line).

the dependence of correlation coefficient on R (details in legends to the figures).

We see from Figs 6 and 7 that if the system is located in a denser environment, it has a greater value of M_{vir}/L ($\alpha < -0.1$, correlation coefficient < -0.3). Moreover, such dependences are true only on scales approximately up to 150–200 kpc for pairs and up to

250–300 kpc for triplets. For greater values of R , the p , t – M_{vir}/L dependences were not observed. This conclusion only confirms our results (Sections 4.2 and 4.3) where we showed that the widest systems most probably are accidental formations, because they do not stand out against a background.

Our results agree with the work of Park, Gott & Yun-Young (2008) who studied the dependence of morphology and luminosity on environment. A strong dependence of morphology on the nearest neighbour was found at distances of about $200 h^{-1}$ kpc. On the other hand, authors (see e.g. Patton et al. 2000; Lambas et al. 2003; Alonso et al. 2004; Woods et al. 2006; De Propriis et al. 2007) on the basis of analysis of physical properties such as star formation rate and colour indices concluded that differences between galaxies in pairs and field galaxies are significant in pairs with $R < 20$ –50 kpc. The dependence on velocity dispersion is weaker, but Lambas et al. (2003) and Alonso et al. (2004) found significant differences in $\Delta V < 100 \text{ km s}^{-1}$.

Because the maximal distance R is a constant, the enhancement of the M_{vir}/L value is a result of the increase in rms velocities in groups. In other words, if the relatively compact pairs and triplets are located in a denser environment, then they have a greater value of mass-to-luminosity ratio due to larger virial motions. The same result was obtained by Einasto et al. (2003). The authors found that loose groups in the neighbourhood of a rich cluster are typically 2.5 times more massive and 1.6 times more luminous than groups on average, and these loose groups have velocity dispersions 1.3 times greater than groups on average.

Table 6 presents the medians and quartiles of system crossing time τ and mass-to-luminosity ratio M_{vir}/L for samples of pairs and triplets that are characterized by different isolation degree and compactness.

From Table 6 it follows that values of M_{vir}/L at $R < 50$ kpc for pairs and $R < 100$ kpc for triplets are 7 – $8 M_{\odot}/L_{\odot}$ and increase with enhancement of R_h faster for triplets than for pairs.

The values of M_{vir}/L are in good agreement with the corresponding values within the IQR for groups that were selected by a dynamical method. The values of M_{vir}/L are $18^{+39}_{-22} M_{\odot}/L_{\odot}$ and $32^{+34}_{-22} M_{\odot}/L_{\odot}$ for pairs and triplets, respectively (Makarov & Karachentsev 2000), and for triplets (from Vavilova et al. 2005) $35^{+30}_{-23} M_{\odot}/L_{\odot}$. The median of most compact triplets is in agreement with the median $M_{\text{vir}}/L = 13^{+16}_{-11} M_{\odot}/L_{\odot}$ obtained for interacting triplets, where the star formation rate is high (Melnyk 2006). The median of isolated triplets is in good agreement with the median $M_{\text{vir}}/L = 47^{+48}_{-33} M_{\odot}/L_{\odot}$ which corresponds to the sample of isolated Northern (Karachentseva, Karachentsev & Sherbanobsky 1979) and Southern (Karachentseva & Karachentsev 2000) triplets.

Table 6. Medians and quartiles of the system crossing time and mass-to-luminosity ratio for pairs and triplets.

| Pairs | N | τ | M_{vir}/L | Triplets* | N | τ | M_{vir}/L |
|-----------|-----|------------------------|--------------------|-----------|-----|------------------------|--------------------|
| $p > Q_3$ | 519 | $1.12^{+1.24}_{-0.59}$ | 12^{+37}_{-10} | $t > Q_3$ | 297 | $1.06^{+0.88}_{-0.42}$ | 44^{+60}_{-28} |
| $R < 50$ | 133 | $0.18^{+0.20}_{-0.07}$ | 7^{+28}_{-6} | $R < 100$ | 16 | $0.24^{+0.07}_{-0.08}$ | 8^{+16}_{-3} |
| $R < 100$ | 335 | $0.40^{+0.47}_{-0.21}$ | 9^{+31}_{-8} | $R < 200$ | 70 | $0.43^{+0.49}_{-0.24}$ | 20^{+46}_{-13} |
| $R < 150$ | 549 | $0.61^{+0.63}_{-0.32}$ | 14^{+44}_{-11} | $R < 300$ | 136 | $0.70^{+0.33}_{-0.28}$ | 24^{+41}_{-16} |
| $R < 200$ | 684 | $0.70^{+0.75}_{-0.34}$ | 17^{+50}_{-14} | $R < 400$ | 240 | $0.71^{+0.39}_{-0.30}$ | 31^{+49}_{-18} |

*Maximal distance R correlates with R_h : $R = 1.41 R_h + 266$; the correlation coefficient is 0.87 for triplets and $R = R_h$ for pairs.

An observable agreement with previous results is additional evidence of the correctness of applying the high-order Voronoi tessellation method for the identification of pairs and triplets.

5 CONCLUSIONS

For the first time we have introduced and applied the high-order 3D Voronoi tessellation method for the identification of isolated galaxies, pairs and triplets.

We used a volume-limited sample of 6786 galaxies from the Northern part of the SDSS DR5 spectroscopic survey ($3000 \leq V_{LG} \leq 9500 \text{ km s}^{-1}$). We selected single galaxies and pairs by the second-order Voronoi tessellation, as well as triplets by the third-order Voronoi tessellation method. As a result we formed 2196 geometric pairs, 1182 triplets and 2394 single galaxies. Then, we introduced parameters p , t and s to characterize the isolation degree of pairs, triplets and single galaxies, respectively. We did not make a clear division between physical gravitationally bound systems and non-physical ones, following the supposition that the more isolated a system is, the higher probability that it is physical. We denoted the subsets of our single galaxies, pairs and triplets with $s < Q_1$, $p > Q_3$ and $t > Q_3$, respectively, as ‘isolated’ (i.e. with the highest isolation degree). The values of quartiles are in Table 1. So, we consider the properties of single galaxies, pairs and triplets in dependence on their isolation degree (in different environments).

Our main conclusions are outlined below.

Compact pairs ($R_h < 150 \text{ kpc}$) and triplets ($R_h < 200 \text{ kpc}$) are more isolated on average than systems in geometric samples, thus they are characterized by different isolation degrees. The wider the pair (triplet), the smaller isolation degree is observed. Small values of parameters p_e and t_e are evidence of a loose environment of these systems (they do not have enough ‘free space’ to be isolated groups). Thus, we consider wide geometric pairs and triplets as accidental ones in the common field.

We compared the luminosities of single galaxies and galaxies in geometric pairs and triplets. It was shown that galaxies in isolated pairs and triplets are two times more luminous than isolated galaxies. On the one hand, it is evidence of the accuracy of our geometric method. On the other hand, we can conclude that in such small groups as pairs and triplets the luminosity–density relation is observed.

We considered the dark matter content in our groups. The median values of M_{vir}/L for our samples limited by different criteria are $12 M_{\odot}/L_{\odot}$ for isolated pairs, $44 M_{\odot}/L_{\odot}$ for isolated triplets and $7 (8) M_{\odot}/L_{\odot}$ for the most compact pairs (triplets) with $R < 50 (100) \text{ kpc}$. Note that for the most compact (close or interacting) systems there is not a very large difference in dark matter content for pairs and triplets, but for isolated triplets the M_{vir}/L is three times larger than for pairs. These results are in agreement with the studies of other authors. We also found that the pair/triplet is a less isolated system (in a denser environment), when M_{vir}/L is greater. This relation testifies that galaxy systems in denser environments have greater rms velocity (because of $M_{\text{vir}} \sim S_v^2$ at fixed distance between galaxies). The p , t – M_{vir}/L dependences are observed only for compact systems (up to 150–200 kpc for pairs and up to 250–300 kpc for triplets).

We conclude that the 3D Voronoi high-order tessellation method is an effective tool for the identification of small groups and the study of their properties in dependence on environment. In our next paper, we will present results on morphological content and colour indices of galaxies in pairs and triplets in comparison with isolated galaxies and their environment.

ACKNOWLEDGMENT

This work was partially supported by the Cosmomicrophysics Program of the NAS of Ukraine. We are also grateful to the Ukrainian Virtual Roentgen and Gamma-Ray Observatory VIRGO.UA, the computing clusters of Main Astronomical Observatory and Bogolyubov Institute for Theoretical Physics, for use of their computing resources.

REFERENCES

- Alonso M. S., Tissera B., Coldwell G., Lambas D., 2004, MNRAS, 352, 1081
- Barrena R., Ramella M., Boschin W., Nonino M., Biviano A., Mediavilla E., 2005, A&A, 444, 685
- Barton E. G., Geller M. J., Kenyon S. J., 2000, ApJ, 530, 660
- Barton E. G., Geller M. J., Kenyon S. J., 2003, ApJ, 582, 668
- Benn C., Wall J., 1995, MNRAS, 272, 678
- Blanton M., Eisenstein D., Hogg D., Schlegel D., Brinkmann J., 2005, ApJ, 629, 143
- Ceccarelli M., Valotto C., Lambas D., Padilla N., Giovanelli R., Haynes M., 2005, ApJ, 622, 853
- Coles P., Barrow J., 1990, MNRAS, 244, 557
- Cooper M., Newman J., Madgwick D., Gerke B., Yan R., Davis M., 2005, ApJ, 634, 833
- Da Rocha C., Ziegler B. L., Mendes de Oliveira C., 2008, MNRAS, 388, 1433
- De Propriis R., Conselice Ch., Liske J., Driver S., Patton D., Graham A., Allen P., 2007, ApJ, 666, 212
- Dressler A., 1980, ApJ, 236, 351
- Ebeling H., Wiedenmann G., 1993, Phys. Rev., 47, 704
- Einasto M., Einasto J., Muller V., Heinamaki P., Tucker D. L., 2003, A&A, 401, 851
- Geller M. J., Kenyon S. J., Barton E. G., Jarrett T. H., Kewley L. J., 2006, AJ, 132, 2243
- Gerke B. F. et al., 2005, ApJ, 625, 6
- Girardi M., Manzato P., Mezzetti M., Giuricin G., Limboz F., 2002, ApJ, 569, 720
- Gomez P. et al., 2003, ApJ, 584, 210
- Gonzales J. A., Quevedo H., Salgado M., Sudarsky D., 2000, A&A, 362, 835
- Icke V., van de Weygaert R., 1987, A&A, 184, 16
- Ikeuchi S., Turner E., 1991, MNRAS, 250, 519
- Jackson J., 1972, MNRAS, 156, 1
- Karachentsev I., 1966, Astrofizika, 2, 81
- Karachentsev I., 1972, Soobshch. Spets. Astrofiz. Obs., 7, 1
- Karachentsev I., 1987, Double Galaxies. Nauka, Moscow (in Russian)
- Karachentseva V., 1973, Soobshch. Spets. Astrofiz. Obs., 8, 3 (KIG)
- Karachentsev I., Makarov D., 1996, AJ, 111, 794
- Karachentseva V. E., Karachentsev I. D., 2000, Astron. Rep., 44, 501
- Karachentsev I. D., Kasparova A. V., 2005, Astron. Lett., 31, 152
- Karachentseva V. E., Karachentsev I. D., Sherbanovsky A. L., 1979, Izv. SAO, 11, 3
- Karachentsev I., Karachentseva V., Lebedev V., 1989, Izv. SAO, 27, 67
- Karachentseva V. E., Melnyk O. V., Vavilova I. B., Makarov D. I., 2005, Kin. Phys. Celest. Bodies, 21, 217
- Kauffmann G., White S., Heckman T., Menard B., Brinchmann J., Charlot S., Tremonti C., Brinkmann J., 2004, MNRAS, 353, 713
- Kiang T., 1966, Z. Astrophys., 64, 433
- Kim R. et al., 2002, AJ, 123, 20
- Lambas D. S., Tissera P. B., Alonso M. S., Coldwell G., 2003, MNRAS, 346, 1189
- Lewis J. et al., 2002, MNRAS, 334, 673
- Lindenbergh R. C., 2002, PhD thesis, Univ. Utrecht
- Lopes P., de Carvalho R., Gal R., Djorgovski S. G., Odewahn S. C., Mahabal A. A., Brunner R. J., 2004, AJ, 128, 1017

- Makarov D. I., Karachentsev I. D., 2000, in Valtonen M. J., Flynn C., eds, ASP Conf. Ser. Vol. 209, Small Galaxy Groups. Astron. Soc. Pac., San Francisco, p. 40
- Makarov D. I., Karachentsev I. D., 2007, in Davies J. I., Disney M. J., eds, Proc. IAU Symp. 244. Cambridge Univ. Press, Cambridge, p. 370
- Marinoni C., Davis M., Newman J., Coil A., 2002, ApJ, 580, 122
- Martinez H., Muriel H., 2006, MNRAS, 370, 1003
- Matsuda T., Shima E., 1984, Prog. Theor. Phys., 71, 205
- Melnyk O. V., 2006, Astron. Lett., 32, 302
- Melnyk O. V., Vavilova I. B., 2006, Kinematika Fiz. Nebesnykh Tel, 22, 422
- Melnyk O. V., Elyiv A. A., Vavilova I. B., 2006, Kinematika Fiz. Nebesnykh Tel, 22, 283
- Mulchaey J., Davis D., Mushotzky R., Burstein D., 2003, ApJS, 145, 39
- Nikolic B., Cullen H., Alexander P., 2004, MNRAS, 355, 874
- Panko E., Flin P., 2006, J. Astron. Data, 12, 1
- Park C., Choi Y., Vogeley S., Gott J., III, Blanton M., 2007, ApJ, 658, 898
- Park C., Gott R., III, Yun-Young C., 2008, ApJ, 674, 784
- Patton D. R., Carlberg R. G., Marzke R. O., Pritchett C. J., da Costa L. N., Pellegrini P. S., 2000, ApJ, 536, 153
- Patton D. R. et al., 2002, AJ, 565, 208
- Patton D. R., Grant J. K., Simard L., 2005, AJ, 130, 2043
- Prada F. et al., 2003, ApJ, 598, 260
- Ramella M., Boschin W., Fadda D., Nonino M., 2001, A&A, 368, 776
- Reda F., Forbes D., Beasley A., O'Sullivan E., Goudfrooij P., 2004, MNRAS, 354, 851
- Soares D. S. L., 2007, AJ, 134, 71
- Stoeck J., Keeney B., Lewis A., Epps H., Schild R., 2004, AJ, 127, 1336
- SubbaRao M., Szalay A., 1992, ApJ, 391, 483
- SubbaRao M., Szalay A., Gulkis S., von Gronfeld P., 1994, ApJ, 420, 474
- Tago E., Einasto J., Saar E., Tempel E., Einasto M., Vennik J., Muller V., 2008, A&A, 479, 927
- Trofimov A. V., Chernin A. D., 1995, AZh, 72, 308
- van de Weygaert R., 1991, MNRAS, 249, 159
- van de Weygaert R., 1994, A&A, 283, 361
- van de Weygaert R., Icke V., 1989, A&A, 213, 1
- van de Weygaert R., Schaap W., 2007, preprint (arXiv:0708.1441v1)
- Vavilova I. B., Karachentseva V. E., Makarov D. I., Melnyk O. V., 2005, Kinematika Fiz. Nebesnykh Tel, 21, 3
- Verley S. et al., 2007, A&A, 472, 121
- Voronoi G., 1908, Reine Angew. Math., 134, 198
- Weinmann S., van den Bosch F., Yang X., Mo H., 2006, MNRAS, 366, 2
- Williams B., Peacock J., Heavens A., 1991, MNRAS, 252, 43
- Woods D. F., Geller M. J., Barton E. J., 2006, AJ, 132, 197
- Xu C. K., Sun Y. C., He X. T., 2004, ApJ, 603, L73
- Zaninetti L., 2006, Chin. J. Astron. Astrophys., 6, 387

APPENDIX A: RADIAL AND PROJECTED DISTANCE

To avoid the fingers-of-God effect, we used the correction factor in the calculation of space distance between galaxies. If the projected r and radial v distances were equivalent, we should calculate a space distance between two galaxies as

$$d^2 = v^2 + r^2. \quad (\text{A1})$$

Obviously, we work in the space of radial velocities and by r we mean $r \times H_0$. We inserted the certain factor $k < 1$ as a weight of the radial component. This factor is responsible for the relative virial motion of galaxies. In that case, the modified distance is $m^2 = v^2 k^2 + r^2$. After some transformations, we obtained the equation of an ellipse:

$$v^2 \frac{k^2}{m^2} + r^2 \frac{1}{m^2} = 1, \quad (\text{A2})$$

where m is the minor semiaxis and $\frac{m}{k}$ is the major semiaxis of the ellipse. We took into account some tolerance v_p in measuring v . For that we labelled the major semiaxis as $\frac{m}{k} = d + v_p$, where d^2 is a distance in the space of radial velocities according to equation (A1). So the weight of the radial component is $k = \frac{m}{d + v_p}$. Since the new distance m is a part of the formula for k , therefore for the simplification we used here $m = d$ and obtained the new distance

$$m^2 = \frac{v^2}{\left(1 + \frac{v_p}{d}\right)^2} + r^2. \quad (\text{A3})$$

In the case of $v_p = 0$, the formula (A3) changes to (A1). If the galaxies are located at a great distance $d \gg v_p$, formula (A3) also changes to (A1). So in these cases, the virial velocities have a weak action on the distance measurement accuracy. If $d \sim v_p$, then $1 + \frac{v_p}{d} > 1$, i.e. the weight of the radial distance decreases. In the case $d \ll v_p$, the denominator $\left(1 + \frac{v_p}{d}\right)^2$ tends to infinity and the radial component loses significance, while the projected distance r keeps it. For our calculations, we used $v_p = 300 \text{ km s}^{-1}$ as the value of typical relative velocities in small galaxy systems (Ceccarelli et al. 2005). Moreover, Karachentsev et al. (1989) showed that the majority of physically bound triplets have rms velocity $S_v < 300 \text{ km s}^{-1}$.

To test the robustness of our method, we compared the main parameters in the cases of different v_p . Table 7 presents the medians and quartiles of S_v and R_h for the obtained galaxy pairs at $v_p = 100$ and 500 km s^{-1} , respectively. The dependences S_v , R_h on v_p are not significant (see Table 2 for comparison). Increasing v_p by five times produces a change of rms velocity and projected distance between galaxies by 1.4 times only. In our paper, we choose the compromise value $v_p = 300 \text{ km s}^{-1}$. So, such an approach lets us avoid the mistaken identification of wide pairs with a small velocity difference.

Table 7. Physical properties of pairs in dependence on isolation parameter and v_p .

| Pairs | N | S_v | R_h |
|-------------------------------|------|------------------|---------------------|
| $v_p = 100 \text{ km s}^{-1}$ | | | |
| All geometric | 2211 | 19^{+15}_{-10} | 399^{+360}_{-219} |
| $p > 2.93$ | 1658 | 17^{+11}_{-9} | 308^{+226}_{-164} |
| $p > 4.72$ | 1005 | 14^{+8}_{-8} | 222^{+163}_{-113} |
| $p > 8.15$ | 553 | 12^{+7}_{-6} | 142^{+92}_{-66} |
| $v_p = 500 \text{ km s}^{-1}$ | | | |
| All geometric | 2210 | 24^{+21}_{-13} | 338^{+331}_{-191} |
| $p > 3.83$ | 1657 | 22^{+17}_{-12} | 237^{+200}_{-120} |
| $p > 6.15$ | 1105 | 20^{+15}_{-10} | 167^{+139}_{-84} |
| $p > 11.19$ | 553 | 17^{+10}_{-9} | 100^{+65}_{-45} |

This paper has been typeset from a \LaTeX file prepared by the author.